

## Thin Film Deposition of Organic–Inorganic Hybrid Materials Using a Single Source Thermal Ablation Technique

D. B. Mitzi,\* M. T. Prikas, and K. Chondroudis

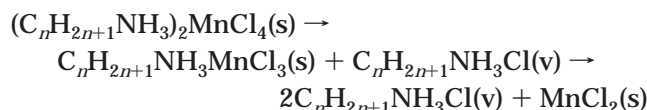
IBM T. J. Watson Research Center, P.O. Box 218,  
Yorktown Heights, New York 10598

Received December 8, 1998

Organic–inorganic superlattice structures have recently attracted substantial attention due to the potential of combining distinct properties of organic and inorganic components within a single molecular composite. The self-assembling organic–inorganic perovskites,<sup>1</sup> for example, adopt an alternating framework of semiconducting inorganic sheets and organic layers. The ability to control the thickness and metal/halogen content of the perovskite sheets and the chemical/physical properties of the organic cations (e.g., length, shape, and polarizability) enables substantial tunability of the natural quantum well structures. Several members of this family exhibit<sup>2,3</sup> a semiconductor–metal transition as a function of increasing perovskite sheet thickness (or well width). Room-temperature photoluminescence,<sup>4,5</sup> third-harmonic generation,<sup>6</sup> and polariton absorption<sup>7</sup> also arise from excitons, with exceptionally large binding energies and oscillator strength, in the inorganic sheets. Recently, a heterostructure electroluminescent (EL) device has been demonstrated<sup>8</sup> employing  $(\text{C}_6\text{H}_5\text{C}_2\text{H}_4\text{NH}_3)_2\text{PbI}_4$  as the active light-emitting component, with intense electroluminescence of more than  $10\,000\text{ cd m}^{-2}$  observed at liquid nitrogen temperature. In addition to the perovskite family, other organic–inorganic hybrids exhibit a range of interesting properties including superconducting transitions,<sup>9</sup> large second-harmonic generation efficiency,<sup>10</sup> and molecular recognition and catalytic properties.<sup>11</sup>

Many studies and potential applications involving the organic–inorganic hybrids depend on the availability of simple and reliable thin film deposition techniques. Deposition of these hybrid materials is often challenging

because of the distinctly different physical and chemical character of the organic and inorganic components. Organic materials, for example, tend to be soluble in different solvents than those appropriate for the inorganic framework, making solution deposition techniques (e.g. spin coating) generally impractical. For those cases where the hybrid is soluble, solution techniques are often not appropriate because of adverse substrate wetting characteristics or the need to uniformly coat an irregular surface. With regard to vacuum deposition techniques, the gradual heating of organic–inorganic composites typically results in the decomposition or dissociation of the organic component at a lower temperature than that required for evaporation of the inorganic component, rendering single source evaporation apparently unfeasible. For example, gradual heating of  $(\text{C}_n\text{H}_{2n+1}\text{NH}_3)_2\text{MnCl}_4$  compounds leads to the two-step dissociation of the organic component from the structure:<sup>12</sup>



Ultimately, if the sample is heated to sufficiently high temperatures, the  $\text{MnCl}_2$  will also melt and evaporate.

Recently, a new dip-processing technique has been demonstrated<sup>13</sup> in which a predeposited metal halide film reacts with organic cations contained in a dipping solution. While this technique is potentially useful for many compounds and applications, the resulting film surfaces are often locally rough and a suitable solvent is required for the dipping process. An entirely vacuum-compatible two-source thermal evaporation technique has also been used to deposit organic–inorganic perovskite films, with separate evaporation sources for the organic and metal halide salts.<sup>14</sup> However, control of the organic salt evaporation rate and therefore balancing of the two deposition rates is difficult to achieve since the organic salt generally does not evaporate as a molecular species, but rather dissociates into the free organic amine and hydrogen halide gas. The resulting films are therefore generally multiphase or defective/disordered as evidenced by extra peaks or the lack of higher order peaks in the X-ray diffraction patterns.

Recently, while sealing organic–inorganic hybrid crystals within an evacuated quartz tube, we observed that traces of the material ablated from the heated tube wall and reassembled as a film of the original hybrid on a cooler section of the tube (as indicated by the characteristic optical properties of the hybrid). This observation suggests the potential for intentionally depositing organic–inorganic films using a single evaporation source, if the hybrid materials are heated sufficiently rapidly. The prototype single source thermal

\* To whom correspondence should be addressed. E-mail: dmitzi@us.ibm.com.

- (1) For a review, see: Mitzi, D. B. *Prog. Inorg. Chem.* **1999**, *48*, 1.
- (2) Mitzi, D. B.; Feild, C. A.; Harrison, W. T. A.; Guloy, A. M. *Nature* **1994**, *369*, 467.
- (3) Mitzi, D. B.; Wang, S.; Feild, C. A.; Chess, C. A.; Guloy, A. M. *Science* **1995**, *267*, 1473.
- (4) Ishihara, T.; Takahashi, J.; Goto, T. *Solid State Commun.* **1989**, *69*, 933.
- (5) Papavassiliou, G. C.; Koutselas, I. B. *Synth. Met.* **1995**, *71*, 1713.
- (6) Calabrese, J.; Jones, N. L.; Harlow, R. L.; Herron, N.; Thorn, D. L.; Wang, Y. *J. Am. Chem. Soc.* **1991**, *113*, 2328.
- (7) Fujita, T.; Sato, Y.; Kuitani, T.; Ishihara, T. *Phys. Rev. B* **1998**, *57*, 12428.
- (8) Era, M.; Morimoto, S.; Tsutsui, T.; Saito, S. *Appl. Phys. Lett.* **1994**, *65*, 676.
- (9) (a) Gamble, F. R.; DiSalvo, F. J.; Klemm, R. A.; Geballe, T. H. *Science* **1970**, *168*, 568. (b) Parkin, S. S. P.; Engler, E. M.; Schumaker, R. R.; Lagier, R.; Lee, V. Y.; Scott, J. C.; Greene, R. L. *Phys. Rev. Lett.* **1983**, *50*, 270.
- (10) Lacroix, P. G.; Clément, R.; Nakatani, K.; Zyss, J.; Ledoux, I. *Science* **1994**, *263*, 658.
- (11) Cao, G.; Garcia, M. E.; Alcalá, M.; Burgess, L. F.; Mallouk, T. E. *J. Am. Chem. Soc.* **1992**, *114*, 7574.

(12) Tello, M. J.; Bocanegra, E. H.; Arrandiaga, M. A.; Arend, H. *Thermochim. Acta* **1975**, *11*, 96.

(13) Liang, K.; Mitzi, D. B.; Prikas, M. T. *Chem. Mater.* **1998**, *10*, 403.

(14) Era, M.; Hattori, T.; Taira, T.; Tsutsui, T. *Chem. Mater.* **1997**, *9*, 8.

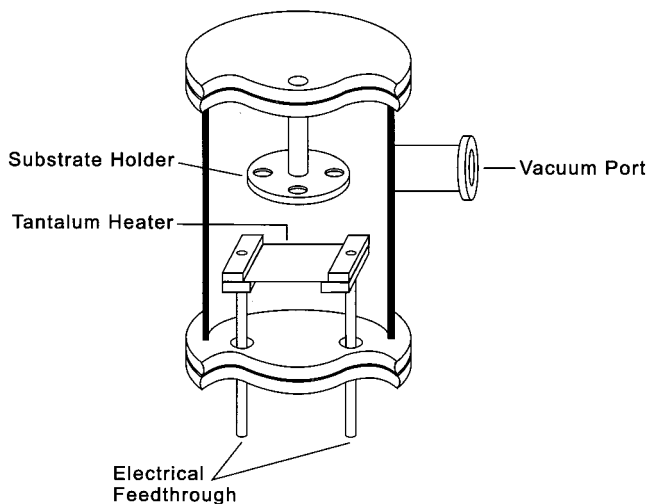


**Figure 1.** Cross sectional view of a typical single source thermal ablation chamber.

ablation (SSTA) apparatus (Figure 1) consists of a vacuum chamber, with an electrical feedthrough to a thin tantalum sheet heater. The heater is positioned directly below a substrate (e.g. quartz, sapphire, glass, plastic, silicon) holder. While other conducting materials can be used for the heater, tantalum is a good choice for the deposition of metal halides since it does not react with these compounds when heated. The starting charge is deposited on the heater in the form of crystals, powder, or a concentrated solution (which is allowed to dry before ablating). Insoluble powders are ideally placed on the heater in the form of a suspension in a quick-drying solvent, since this enables the powder to be in better physical and thermal contact with, as well as more evenly dispersed across, the sheet. After establishing a suitable vacuum, a large current is passed through the tantalum sheet. While the sheet temperature reaches approximately 1000 °C in 1–2 s, the entire starting charge ablates from the heater surface well before it incandesces. The rate of heating during the ablation process is therefore more critical than the ultimate temperature achieved. The organic and inorganic components reassemble on the substrates after ablation to produce optically clear films of the desired product.

A number of organic–inorganic hybrids have been deposited using this technique, including  $(\text{C}_6\text{H}_5\text{C}_2\text{H}_4\text{NH}_3)_2\text{PbI}_4$ ,  $(\text{C}_6\text{H}_5\text{C}_2\text{H}_4\text{NH}_3)_2\text{PbBr}_4$ , and  $(\text{C}_4\text{H}_9\text{NH}_3)_2\text{SnI}_4$ . These examples demonstrate that among the strongly luminescent organic–inorganic perovskites, the technique can be used for a range of organic cations and inorganic frameworks. For each compound, approximately 15 mg of the organic–inorganic perovskite (synthesized using standard techniques<sup>1</sup>) is dissolved in 1 mL of anhydrous *N,N*-dimethylformamide (DMF). For  $(\text{C}_6\text{H}_5\text{C}_2\text{H}_4\text{NH}_3)_2\text{PbI}_4$  and  $(\text{C}_4\text{H}_9\text{NH}_3)_2\text{SnI}_4$ , the best results are achieved using a stoichiometric starting solution. For  $(\text{C}_6\text{H}_5\text{C}_2\text{H}_4\text{NH}_3)_2\text{PbI}_4$ , however, better results have been achieved by including a small excess of phenethylammonium iodide in the initial solution [for example, 15 mg of  $(\text{C}_6\text{H}_5\text{C}_2\text{H}_4\text{NH}_3)_2\text{PbI}_4$  and 2 mg of  $\text{C}_6\text{H}_5\text{C}_2\text{H}_4\text{NH}_2\cdot\text{HI}$ ]. A small volume (0.1–0.4 mL) of the solution is dried on the 0.025 mm thick tantalum foil (which is positioned approximately 8 cm below the substrates). After pumping the chamber to  $<10^{-4}$  Torr,

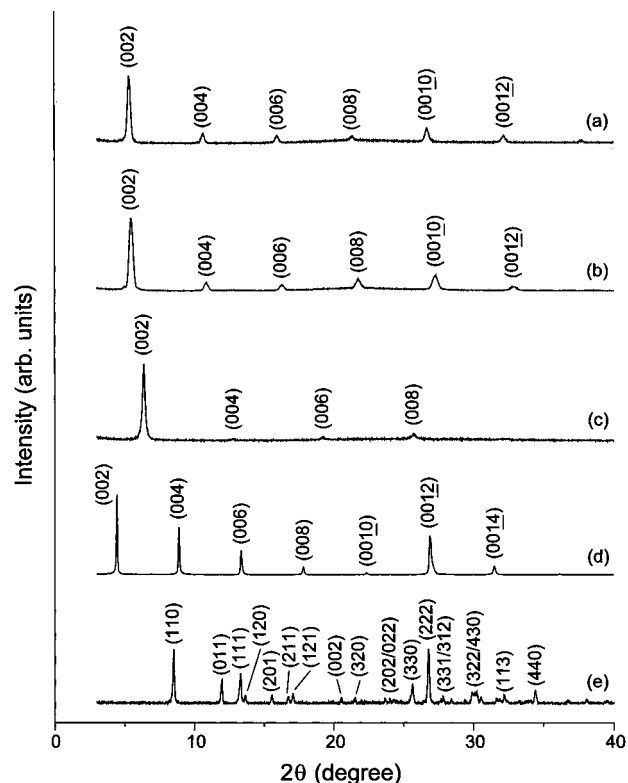


**Figure 2.** Room-temperature X-ray diffraction patterns for films of the organic–inorganic perovskites (a)  $(\text{C}_6\text{H}_5\text{C}_2\text{H}_4\text{NH}_3)_2\text{PbBr}_4$ , (b)  $(\text{C}_6\text{H}_5\text{C}_2\text{H}_4\text{NH}_3)_2\text{PbI}_4$ , (c)  $(\text{C}_4\text{H}_9\text{NH}_3)_2\text{SnI}_4$ , and (d)  $(\text{C}_4\text{H}_9\text{NH}_3)_2(\text{CH}_3\text{NH}_3)\text{Sn}_2\text{I}_7$ , deposited using the SSTA technique. The *c* axis lattice parameters derived from the X-ray patterns are 33.37(2), 32.65(2), 27.64(2), and 39.72(2) Å, respectively, and are in agreement with published values.<sup>1</sup> (e) The X-ray diffraction pattern for  $\text{NH}_3(\text{CH}_2)_6\text{NH}_3\text{BiI}_5$  demonstrates that the SSTA-deposited films of this material are less crystallographically oriented on the substrate compared to the layered perovskite films.

the vacuum valve is closed, thereby isolating the chamber from the pump. A current of 80–90 A is passed through the heater sheet for 2–5 s, ablating the hybrid on the heater. The resulting film thickness after ablation (from 10 to >200 nm) is controlled by selecting the initial volume of material placed on the heater. An atomic force microscope (AFM) study of a  $(\text{C}_6\text{H}_5\text{C}_2\text{H}_4\text{NH}_3)_2\text{PbI}_4$  film surface demonstrates a mean roughness of approximately 1.6 nm, similar to the values observed for spin-coated films of the same material.<sup>13</sup> The thermally ablated film also exhibits a relatively small (<75 nm) grain size.

Figure 2a–c shows X-ray diffraction patterns for each of the three perovskites deposited using the thermal ablation process. In each case, the single-phase films are highly oriented [i.e., only (00*l*) reflections are observed], with the plane of the perovskite sheets parallel to the substrate surface. The existence of a number of higher order (00*l*) reflections indicates that the films are well-crystallized, with diffraction peak widths (fwhm) generally in the range 0.25–0.45°, depending on deposition conditions and ultimate film thicknesses. The slightly broadened peaks are consistent with the generally small grain size (as observed in the AFM study). The luminescence spectra for the three deposited perovskite films are also shown in Figure 3. The strong sharp peak in each spectrum corresponds

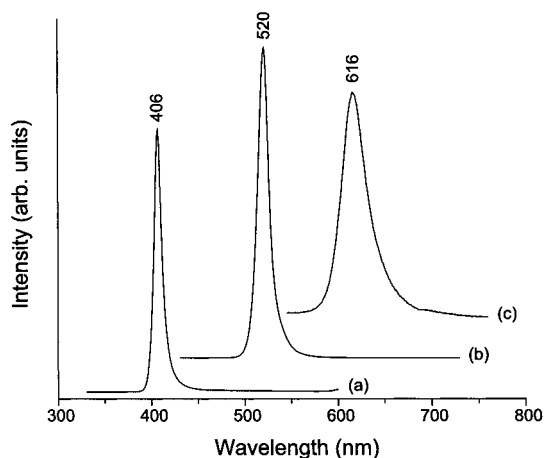


**Figure 3.** Room-temperature photoluminescence spectra for (a)  $(\text{C}_6\text{H}_5\text{C}_2\text{H}_4\text{NH}_3)_2\text{PbBr}_4$ , (b)  $(\text{C}_6\text{H}_5\text{C}_2\text{H}_4\text{NH}_3)_2\text{PbI}_4$ , and (c)  $(\text{C}_4\text{H}_9\text{NH}_3)_2\text{SnI}_4$  films, deposited on quartz using the SSTA technique. Each spectrum was recorded using a SPEX Fluorolog-2 spectrometer with a xenon arc lamp excitation source. The films were excited at 307, 379, and 430 nm, respectively.

to the radiative decay of excitons within the inorganic sheets of the perovskite structure and again demonstrates the high quality of the films.

Note that the rapid nature of the ablation process appears to be an important component of this vacuum evaporation technique. If the rate of the evaporation from the heater sheet is reduced (i.e. the heater power is turned down), the deposited films no longer consist of a single phase. For example, in the deposition of  $(\text{C}_6\text{H}_5\text{C}_2\text{H}_4\text{NH}_3)_2\text{PbBr}_4$  films, reducing the heater current to 55 A (which provides for complete evaporation in  $\sim 30$  s) yields films which are primarily a mixture of crystalline  $\text{C}_6\text{H}_5\text{C}_2\text{H}_4\text{NH}_2 \cdot \text{HBr}$  and a nominally amorphous  $\text{PbBr}_2$  phase. Upon annealing at 100 °C, the correct perovskite structure forms along with a small amount of  $\text{PbBr}_2$ . While the more gradual evaporation process still enables most of the organic and inorganic components to reach the substrate, faster ablation is apparently important for achieving single phase films (at least without annealing), perhaps because this enables both the organic and inorganic components to reach the substrate at effectively the same time.

The SSTA process also addresses the problem of depositing mixed-organic hybrid systems since, regardless of the volatility of each component, everything on the heater sheet ablates virtually simultaneously. To demonstrate this point, the more three-dimensional semiconducting perovskite,  $(\text{C}_4\text{H}_9\text{NH}_3)_2(\text{CH}_3\text{NH}_3)\text{Sn}_2\text{I}_7$ , has been successfully deposited using a similar process to that described above. The film used for the X-ray diffraction pattern in Figure 2d was generated using two identical and successive ablation cycles, thereby providing for a thicker film with a sharper X-ray diffraction profile. The derived *c* axis lattice parameter reflects the

inclusion of one extra perovskite sheet between each set of butylammonium bilayers [relative to  $(\text{C}_4\text{H}_9\text{NH}_3)_2\text{SnI}_4$ ]. To further highlight the versatility of the SSTA technique, thin films of the nonperovskite  $\text{NH}_3(\text{CH}_2)_6\text{NH}_3\text{BiI}_5$  have also been deposited. The  $\text{NH}_3(\text{CH}_2)_6\text{NH}_3\text{BiI}_5$  structure<sup>15</sup> consists of a framework of quasi-one-dimensional  $\text{BiI}_5^{2-}$  chains separated by the organic cations. The absorption spectra of SSTA-deposited  $\text{NH}_3(\text{CH}_2)_6\text{NH}_3\text{BiI}_5$  films are identical to that previously reported for the compound.<sup>15</sup> The films are also less crystallographically oriented (see Figure 2e) than the two-dimensional superlattice films formed by the layered perovskites.

In summary, we have demonstrated that a substantial range of organic–inorganic hybrids can be ablated at temperatures high enough for the inorganic component to quickly evaporate, without the organic component thermally decomposing. The reorganization (or self-assembly) of the organic and inorganic components into the organic–inorganic hybrid after ablation generally occurs on the substrate during the deposition process, without the need for postprocessing (e.g. annealing) of the films. In contrast to other established techniques<sup>1</sup> (e.g. spin coating, two-source thermal evaporation, and dip processing), single source thermal ablation offers the ability to expeditiously produce high-quality films, without the need to find a suitable solvent for the hybrid (one that both dissolves the hybrid and wets the substrate surface) or to balance deposition rates from multiple evaporation sources. The rapid nature of the ablation process enables a quick turn-around time and also relaxes the need for stringent vacuum conditions. The SSTA process is similar in concept to laser ablation, which has been used to deposit a number of multicomponent inorganic films. In contrast to laser ablation, however, which might lead to photodegradation of the organic molecules, heating is generated by passing a current through a resistive sheet. The high quality of the resulting films and the ability to pattern the films during the deposition process suggests the applicability of the SSTA process for fabricating devices. Preliminary LEDs incorporating patterned SSTA-deposited  $(\text{C}_6\text{H}_5\text{C}_2\text{H}_4\text{NH}_3)_2\text{PbX}_4$  (*X* = Br and I) exhibit strong electroluminescence at liquid nitrogen temperature.<sup>16</sup>

**Acknowledgment.** The authors gratefully acknowledge DARPA for partial support of this work under contract DAAL01-96-C-0095, David Abraham for performing AFM measurements, and Cherie Kagan for a careful reading of the manuscript.

CM9811139

(15) Mousdis, G. A.; Papavassiliou, G. C.; Terzis, A.; Raptopoulou, C. P. *Z. Naturforsch.* **1998**, *53b*, 927.

(16) Chondroudis, K.; Mitzi, D. B.; Prikas, M. T. Unpublished.